Linear and Nonlinear Optical Response of $LiNbO_3$ Calculated From First Principles

Arthur Riefer, Simone Sanna, Alexander V. Gavrilenko, and Wolf Gero Schmidt

***Abstract*—The dielectric function and second-harmonic generation spectrum of ferroelectric $LiNbO_3$ are calculated from first principles. The calculations are based on the electronic structure obtained within density functional theory. The use of the *GW* approach to account for quasiparticle effects and the subsequent solution of the Bethe–Salpeter equation lead to a dielectric function in excellent agreement with measured data. The second harmonic generation spectrum calculated within the independent (quasi) particle approximation predicts strong nonlinear coefficients for photon energies above about 1.5 eV. The comparison with measured data suggests that the inclusion of self-energy effects in the nonlinear response improves the agreement with experiment.**

LITHIUM niobate ($LiNbO_3$, LN) occurs in two phases of trigonal symmetry with ten atoms per unit cell. The ground-state is ferroelectric with space group $R3c$. Its electro-optic, photo-refractive, and nonlinear optical properties (cf. [1], [2]) are exploited in a large number of devices. Typical uses are in optical modulators, acousto-optic devices, optical switches for gigahertz frequencies, laser frequency doubling, nonlinear optics, Pockels cells, optical parametric oscillators, or Q-switching devices for lasers.

Given its vast range of applications, our knowledge about the electronic and optical properties of LN is surprisingly limited. For example, we are not aware of a measured band structure. The direct band gap of 3.78 eV for the ferroelectric phase—frequently cited in the literature—is actually concluded from optical experiments [3]. Therefore, it is affected by electron-hole attraction effects which may substantially reduce the size of the actual band gap, i.e., the difference between the ionization energy and the electron affinity. The situation is additionally complicated by the fact that there are actually several band gap values reported, all concluded from optical absorption experiments. They range from the indirect gap of 3.28 eV reported in [4] to values of 4.0 or 4.3 eV [5], [6]. Recent theoretical work suggests that the actual band gap is substantially larger, of the order of 4.7 to 6.5 eV [7], [8].

Manuscript received January 6, 2012; accepted May 25, 2012. The calculations were done using grants of computer time from the Paderborn Center for Parallel Computing (PC^2) and the Höchstleistungs-Rechenzentrum Stuttgart. The Deutsche Forschungsgemeinschaft is acknowledged for financial support.

A. Riefer, S. Sanna, and W. G. Schmidt are with the Lehrstuhl für Theoretische Physik, Universität Paderborn, Paderborn, Germany (e-mail: simone.sanna@uni-paderborn.de).

A. V. Gavrilenko is with Norfolk State University, Center for Materials Research, Norfolk, VA.

DOI http://dx.doi.org/10.1109/TUFFC.2012.2409

The previously mentioned optical absorption experiments, as well as further studies, e.g [9], focus mainly on the onset of the absorption. We are aware of only two studies that address the linear optical absorption in the vacuum ultraviolet (VUV) domain [10], [11]. Second-harmonic generation (SHG) data for a few fundamental frequencies have been published, e.g., in [12]–[15]. We are not aware of SHG measurements covering a wide spectral range.

In recent years, several first-principles studies have become available on the structural and vibrational properties of bulk LN, see, e.g., [7], [16]–[18]. The structural and vibrational properties of LN surfaces have also been addressed by atomistic simulations [19]–[21]. The phase transition between paraelectric and ferroelectric LN was modeled with molecular dynamics [22]. Comparatively few calculations were performed on the optical and electronic properties of LN. Most first-principles band-structure calculations, e.g., [18], [23], are based on a single-particle framework and neglect quasiparticle effects that typically widen the band gap between occupied and empty states by a large fraction of its value [24]. An early theoretical study by Ching *et al.* [25] indicates the importance of self-energy effects: Using the approximate Sterne–Inkson model [26], they predicted self-energy corrections of the order of 1 eV. However, the single-particle gap in [25] is much smaller (2.62 eV for the ferroelectric phase) than in the more recent studies [23] (3.69 eV) and [18] (3.48 eV). Schmidt *et al.* [7] found indications for a very strong influence of excitonic and local-field effects on the LN optical absorption. Although the calculations in [7] explain the essential features of the measured optical absorption [10], [11], their predictive power is limited, because of the use of a model dielectric function [27] for the description of the screened Coulomb interaction W in the GW approximation. In particular, the possible influence of lattice polarization effects [28] on the LN electronic and optical excitations could not be satisfactorily clarified in [7]. Although approximate analytical schemes [29] and density functional theory (DFT) pseudopotential calculations [30] were used to calculate SHG spectra, the influence of many-body effects on the nonlinear optical properties of LN has not been studied yet.

The present work goes significantly beyond previous theoretical work because, for the first time, the self-energy effects in the linear and nonlinear optical spectra are addressed from first principles, i.e., quasi-particle corrections were calculated in the GW approach (GWA) [31] using the random phase approximation to describe the screened Coulomb potential.

The calculation of the optical absorption occurs in three steps: 1) We use density functional theory in generalized gradient approximation (DFT-GGA) to determine the electronic ground state of ferroelectric LN; 2) the electronic quasiparticle spectrum is obtained within the GWA to model the exchange-correlation self-energy; and, finally, 3) the Bethe–Salpeter equation (BSE) is solved for coupled electron-hole excitations [32]–[34], thereby accounting for the screened electron-hole attraction and the unscreened electron-hole exchange [35]–[37].

In detail, we start from first-principles projector augmented wave (PAW) calculations, using the VASP implementation of the DFT-GGA [38], [39]. A $6 \times 6 \times 6$ **k**-point mesh is used to sample the Brillouin zone. The electron wave functions are expanded into plane waves up to an energy cutoff of 400 eV. The mean-field effects of exchange and correlation in GGA are modeled using the PW91 functional [40].

In the second step, we include electronic self-energy effects by a perturbative solution of the quasiparticle equation, where the GGA exchange and correlation potential is replaced by the nonlocal and energy-dependent self-energy operator Σ. We calculate Σ in the G_0W_0 approximation [31]—using the implementation described in [41]—from the convolution of the single-particle propagator G and the dynamically screened Coulomb interaction W. Thereby, 608 electronic bands were included in the calculation of the self-energy operator.

The electron-hole interaction is taken into account in the third step. The two-particle Hamiltonian

$$\begin{aligned} H_{vck,v'c'k'} &= (\varepsilon_{ck} - \varepsilon_{vk})\delta_{vv'}\delta_{cc'}\delta_{k,k'} \\ &\quad + 2\iint \mathrm{d}r\mathrm{d}r'\psi^*_{ck}(r)\psi_{vk}(r)\overline{v}(r-r')\psi_{c'k'}(r')\psi^*_{v'k'}(r') \\ &\quad - \iint \mathrm{d}r\mathrm{d}r'\psi^*_{ck}(r)\psi_{c'k'}(r)W(r,r')\psi_{\boldsymbol{vk}}(r')\psi^*_{v'k'}(r'), \end{aligned} \tag{1}$$

describes the interaction of pairs of electrons in conduction states $|ck\rangle$ and holes in valence states $|vk\rangle$ [35]–[37]. The diagonal first part is given by the quasiparticle energies obtained in G_0W_0 approximation. The second, the electron-hole exchange term, in which the short-range part of the bare Coulomb potential $\overline{v}$ enters, reflects the influence of local fields. Finally, the third part, which describes the screened electron-hole attraction, is calculated using the model dielectric function proposed by Bechstedt *et al.* [27]. Thereby, we use the value $\varepsilon_\infty = 6.13$ calculated within the independent-particle approximation (IPA) as input parameter. For the actual calculation of the polarizability, we use the time-evolution implementation described in [42] and [43].

The present SHG calculations neglect intraband contributions and approximate the non-linear response from interband transitions according to the expression derived, e.g., in [44],

$$\begin{aligned} \chi^{(2)}_{abc}(-2\omega,\omega,\omega) &= -\frac{ie^3}{m^3\hbar^2 V}\sum_{nmlk}{}' \frac{p^a_{nm}(k)\{p^b_{ml}(k)p^c_{ln}(k)\}}{\omega_{ln}(k)-\omega_{ml}(k)} \\ &\quad \times\Bigg[\frac{16 f_{nm}(k)}{[\omega_{mn}(k)]^3[\omega_{mn}(k)-2\tilde{\omega}]} \\ &\quad + \frac{f_{ml}(k)}{[\omega_{ml}(k)]^3[\omega_{ml}(k)-\tilde{\omega}]} \\ &\quad + \frac{f_{ln}(k)}{[\omega_{ln}(k)]^3[\omega_{ln}(k)-\tilde{\omega}]}\Bigg], \end{aligned} \tag{2}$$

where

$$\{p^b_{ml}(k)p^c_{ln}(k)\} = \frac{1}{2}[p^b_{ml}(k)p^c_{ln}(k) + p^c_{ml}(k)p^b_{ln}(k)], \tag{3}$$

and f_{nm} and p^a_{nm} are the Fermi blocking factors and $a = x, y, z$ component of the momentum matrix elements, respectively, for the respective Bloch states n and m. $\tilde{\omega} = \omega + i\eta$ denotes the photon frequency ω with a small positive imaginary part η, which turns off the electromagnetic field adiabatically. The energy difference between band m and n at point **k** in the Brillouin zone is given by $\hbar\omega_{mn}(k) = \varepsilon_{mk} - \varepsilon_{nk}$. Eq. (3) has been used to calculate the SHG spectra of LN within the IPA and independent-quasiparticle approximation (IQA) using the electronic structure obtained from either the DFT calculations and the self-energies from the GWA, respectively.

Calculated SHG data are known to be rather sensitive with respect to numerical details such as the number of **k** points used to sample the Brlllouin zone and the number of electronic bands included in the calculation [45]. Here, the uppermost 18 valence bands and the lowest 34 conduction bands were taken into account. Fig. 1 shows that the application of a $6 \times 6 \times 6$ **k**-point mesh is sufficient to obtain converged results for the linear and nonlinear spectra. The inclusion of excitonic effects in the SGH calculations was, for numerical reasons, beyond the scope of the present study.

The electronic band structure and density of states of ferroelectric $LiNbO_3$ as calculated here within the DFT and within the GWA are shown in Fig. 2. In our calculations, LN appears to have an indirect band gap, with the valence band maximum slightly off the Γ point. However, the uppermost valence band is relatively flat, so that the difference between the direct and indirect gap is lower than 0.1 eV. Although the direct band gap at Γ of 3.39 eV calculated here within DFT agrees well with previous calculations on the same level of theory [7], [18], [23], the comparison of the present G_0W_0 value of 5.42 eV with earlier calculations requires some care. The authors of [7] used a model dielectric function to describe the screened Coulomb interaction in the self-energy operator. This may, on one hand, impair the accuracy of the calculations; on the other hand, it provides a simple means to access, to some extent, the influence of the lattice polarizability on

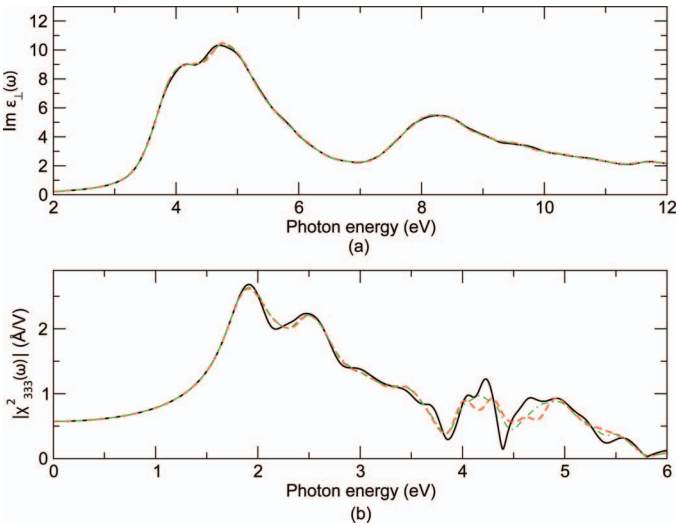

Fig. 1. Imaginary part of the dielectric function (a) for ordinary (perpendicular to c, $\varepsilon_\perp$) polarization and (b) zzz component of the absolute value of the nonlinear spectrum of ferroelectric lithium niobate calculated within the independent-particle approximation (IPA) with a (solid line) $6 \times 6 \times 6$, (dashed line) $8 \times 8 \times 8$, and (dotted line) $10 \times 10 \times 10$ **k**-point mesh. A broadening of $\eta = 0.2$ eV is applied.

the quasiparticle energies [28]. Depending on whether or not the lattice is supposed to contribute to the screening, a fundamental band gap between about 6.5 and 5.4 eV is predicted for ferroelectric LN in [7]. The present G_0W_0 calculations do not include any lattice polarization effects, and should thus be compared with the 6.5 eV obtained in [7]. The deviation of about 1 eV in the predicted band gaps is an indication that the screening in the strongly ionic material studied here is not satisfactorily described by a model dielectric function. However, previous first-principles GW calculations [8] using the full-potential linearized augmented plane-wave method predict a gap value of about 4.7 eV for ferroelectric LN. This value is 0.7 eV smaller than the band gap calculated in the present work. This deviation is somewhat larger than typically expected for converged GW calculations. We are presently investigating the origin of this discrepancy. The comparison of the measured and calculated optical response below suggests, however, that the present G_0W_0 value of about 5.4 eV is close to the actual value.

The electronic band structure shown in Fig. 2 is the basis for the optical response calculations. In Fig. 3, we show the linear optical response calculated for ferroelectric LN according to the three levels of theory, i.e., IPA (DFT), IQA (GWA), and BSE. The spectrum obtained within the IPA for ferroelectric LN agrees roughly with earlier independent-particle results [23], [25]. There are two main features of the optical absorption centered at about 5 and 8 eV that arise from transitions between O $2p$ and Nb $4d$ states (cf. Fig. 2(b) and [7]). The inclusion of the many-body interaction in the electronic structure (IQA), leads to a nearly rigid blueshift of the spectra by about 2 eV. The Coulomb correlation of electrons and holes, accounted for by solving the BSE, changes the line shape somewhat. The first peak of the low-energy main feature of the optical absorption becomes more pronounced and the whole feature is redshifted compared with the IQA spectrum. It is now positioned at 5.5 or 5.6 eV for $\varepsilon_\perp$ or $\varepsilon_{||}$, respectively. The oscillator strength of the originally rather broad (~2 eV) high-energy main feature of the optical absorption is redshifted and transferred into a single sharp peak at about 9.3 eV (for $\varepsilon_\perp$ or $\varepsilon_{||}$). Based on the orbital character of the electronic states contributing to the respective peaks in the IPA spectrum [cf. also Fig. 2(b)] it is very likely that the strong localization of the states responsible for both the first and the second absorption peak causes the strong excitonic effects in both cases. Unfortunately, our time-evolution-based BSE implementation does not allow access to single excitonic states to address the origin of the two peaks unambiguously.

Compared with the experimental data for ferroelectric LN, in which absorption features at 5.3 to 6 eV and 9.2 to 10 eV are observed [10], [11], the inclusion of self-energy and excitonic effects substantially improves the theoretical description. This concerns both the peak positions and the line shapes, which sharpen because of the inclusion of excitonic effects. Consequently, the experimental observation that the first absorption peak is broader for $\varepsilon_{||}$ than for $\varepsilon_\perp$ in ferroelectric LN [11] is reproduced in the calculations that account for electron-hole interactions much more clearly than on the single-particle level of theory. The detailed comparison of the measured and calculated onset of the optical absorption shows that the simulated spectra are blue shifted by about 0.1 to 0.2 eV. The lineshape of the calculated spectra presented here agrees somewhat better with experiment than the previous calculation in [7], which we trace back to the more accurate description of the self-energy effects in the GW calculation. The inclusion of lattice polarization effects (neglected here) in the calculations is expected to redshift the calculated absorp-

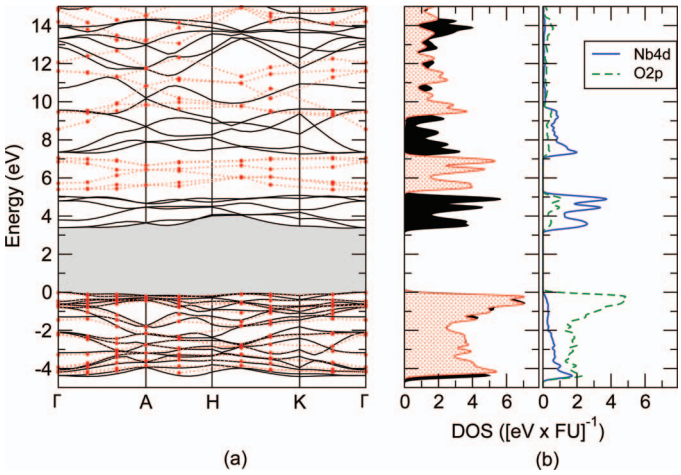

Fig. 2. (a) Electronic band structure (with respect to the valence band maximum, for the notation of high symmetry points see, e.g., [7, Fig. 3]) and (b) density of states (DOS) [in 1/eV per lithium niobate (LN) formula unit (FU)] of ferroelectric LN calculated within (solid lines, black) DFT-PW91 and (red circles, dotted region) G_0W_0. Dotted lines guide the eye. The fundamental gap is indicated in gray. Also shown in (b) are the contributions of Nb $4d$ and O $2p$ states to the DOS calculated within DFT-PW91.

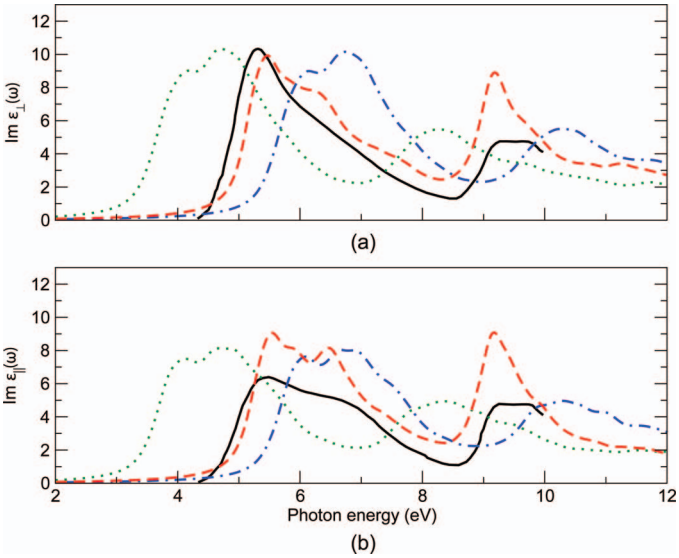

Fig. 3. Imaginary part of the dielectric function of ferroelectric lithium niobate for (a) ordinary (perpendicular to c, $\varepsilon_{\perp}$) and (b) extraordinary (parallel to c, $\varepsilon_{||}$) polarization calculated within the (dotted line) independent-particle approximation (IPA), (dot-dashed line) independent-quasiparticle approximation (IQA), and (dashed line) Bethe–Salpeter equation (BSE) (with G_0W_0 corrections) compared with (solid line) experimental measurements of [11].

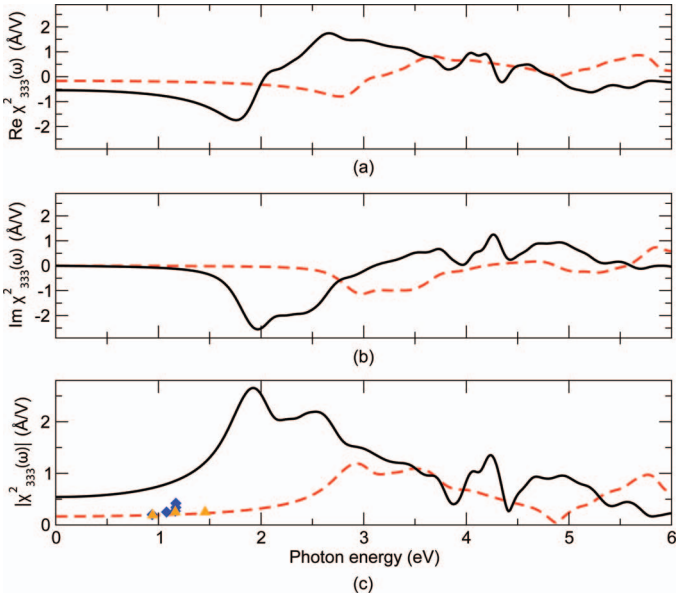

Fig. 4. (a) Real part, (b) imaginary part, and (c) absolute value of χ^2_{333} of ferroelectric lithium niobate calculated within the (solid line) independent-particle approximation (IPA) and (dashed line) independent-quasiparticle approximation (IQA). Diamonds and triangles in (c) denote experimental values from [15, Tables 2 and 6].

tion features [7]. The present findings may therefore be interpreted as an indication that the lattice polarizability influences, to some extent, the single- and two-particle electronic excitations in LN. On the other hand, it should be mentioned that the many-body techniques employed here have intrinsic uncertainties of just this order of magnitude.

In Fig. 4, we present the *zzz* component of the SHG spectrum of ferroelectric LN calculated within the IPA and IQA. Shown are the real part, imaginary part, and absolute value of $\chi^2_{333}(\omega)$ up to 6 eV. The IPA results show two main features between 1.5 to 3.0 eV and 3.8 to 4.4 eV. As expected from the structure of (2), the shift of the spectral features resulting from the inclusion of self-energy effects differs from the GW band gap correction. We observe a shift of about 1 eV in the SHG features if quasiparticle effects are included from the GW calculations. Also, the magnitude of the nonlinearities is lower in the IQA results. Experimentally, absolute values $|\chi^2_{333}|$ between 0.2 to 0.4 Å/V for photon energies around 1 eV [15] are reported. The comparison with the calculated spectra on IPA and IQA levels of theory (Fig. 4) shows that the former overestimate the measured data, whereas the IQA calculations that include electronic self-energy effects describe the optical nonlinearities well. However, because measured SHG values are available only for a few fundamental wavelengths and the calculated spectra neither account for intraband transitions nor for electron-hole interaction, at this point, no definite conclusions should be drawn from the comparison between experiment and theory. Particularly, excitonic effects may have a noticeable influence on the SHG spectra as stated by Luppi *et al.* [46] studying the GaAs nonlinear spectra.

To summarize, first-principles calculations of the $LiNbO_3$ linear and nonlinear optical properties are performed. The calculated optical absorption spectrum including electron-hole and self-energy effects is in excellent agreement with the measured data. Strong exciton binding energies of the order of 1 eV are predicted. The slight underestimation of the optical absorption onset in the calculations may indicate lattice polarizability contributions to the screening of one- and two-particle excitations in LN. The calculated SHG spectrum shows noticeable nonlinearities for photon energies above 1.5 eV. The comparison with experiment indicates that the inclusion of self-energy effects in SHG spectra substantially improves the agreement between measured and calculated data.

References

[1] A. Räuber, "Chemistry and physics of lithium niobate," *Curr. Topics Mater. Sci.*, vol. 1, pp. 481–601, 1978.

[2] R. S. Weis and T. K. Gaylord, "Lithium niobate: Summary of physical properties and crystal structure," *Appl. Phys. A*, vol. 37, no. 4, pp. 191–203, 1985.

[3] A. Dhar and A. Mansingh, "Optical properties of reduced lithium niobate single crystals," *J. Appl. Phys.*, vol. 68, no. 11, pp. 5804–5809, 1990.

[4] Z. Jiangou, Z. Shipin, X. Dingquan, W. Xiu, and X. Guanfeng, "Optical absorption properties of doped lithium niobate crystals," *J. Phys. Condens. Matter*, vol. 4, no. 11, pp. 2977–2983, 1992.

[5] D. Redfield and W. J. Burke, "Optical absorption edge of $LiNbO_3$," *J. Appl. Phys.*, vol. 45, no. 10, pp. 4566–4571, 1974.

[6] S. Kase and K. Ohi, "Optical absorption and interband faraday rotation in $LiTaO_3$ and $LiNbO_3$," *Ferroelectrics*, vol. 8, no. 1, pp. 419–420, 1974.

[7] W. G. Schmidt, M. Albrecht, S. Wippermann, S. Blankenburg, E. Rauls, F. Fuchs, C. Rödl, J. Furthmüller, and A. Hermann, "$LiNbO_3$ ground- and excited-state properties from first-principles calculations," *Phys. Rev. B*, vol. 77, art. no. 035106, 2008.

[8] C. Thierfelder, S. Sanna, A. Schindlmayr, and W. G. Schmidt, "Do we know the band gap of lithium niobate?" *Phys. Stat. Sol. C*, vol. 7, no. 2, pp. 362–365, 2010.

[9] H. Li, G. Xu, G. Hu, and X. Wang, "Effect of dopant Zn on the optical absorption properties of lithium niobate crystals," *Cryst. Res. Technol.*, vol. 29, no. 5, pp. 693–696, 1994.
[10] A. M. Mamedov, M. A. Osman, and L. C. Hajieva, "VUV reflectivity of $LiNbO_3$ and $LiTaO_3$ single crystals," *Appl. Phys., A*, vol. 34, no. 3, pp. 189–192, 1984.
[11] E. Wiesendanger and G. Güntherodt, "Optical anisotropy of $LiNbO_3$ and $KNbO_3$ in the interband transition region," *Solid State Commun.*, vol. 14, no. 4, pp. 303–306, 1974.
[12] R. C. Miller, W. A. Nordland, and P. M. Bridenbaugh, "Dependence of second-harmonic-generation coefficients of $LiNbO_3$ on melt composition," *J. Appl. Phys.*, vol. 42, no. 11, pp. 4145–4147, 1971.
[13] M. M. Choy and R. L. Byer, "Accurate second-order susceptibility measurements of visible and infrared nonlinear crystals," *Phys. Rev. B*, vol. 14, pp. 1693–1706, Aug. 1976.
[14] R. C. Eckardt, H. Masuda, Y. X. Fan, and R. L. Byer, "Absolute and relative nonlinear optical coefficients of KDP, KD*P, BaB_2O_4, $LiIO_3$, MgO:$LiNbO_3$, and KTP measured by phase-matched second-harmonic generation," *IEEE J. Quant. Electron.*, vol. 26, pp. 922–933, May 1990.
[15] I. Shoji, T. Kondo, A. Kitamoto, M. Shirane, and R. Ito, "Absolute scale of second-order nonlinear-optical coefficients," *J. Opt. Soc. Am. B*, vol. 14, p. 2268–2294, Sep. 1997.
[16] V. Caciuc, A. V. Postnikov, and G. Borstel, "*Ab initio* structure and zone-center phonons in $LiNbO_3$," *Phys. Rev. B*, vol. 61, pp. 8806–8813, Apr. 2000.
[17] K. Parlinski, Z. Q. Li, and Y. Kawazoe, "*Ab initio* calculations of phonons in $LiNbO_3$" *Phys. Rev. B*, vol. 61, pp. 272–278, Jan. 2000.
[18] M. Veithen and P. Ghosez, "First-principles study of the dielectric and dynamical properties of lithium niobate," *Phys. Rev. B*, vol. 65, art. no. 214302, May 2002.
[19] S. V. Levchenko and A. M. Rappe, "Influence of ferroelectric polarization on the equilibrium stoichiometry of lithium niobate (0001) surfaces," *Phys. Rev. Lett.*, vol. 100, art. no. 256101, Jun. 2008.
[20] S. Sanna and W. G. Schmidt, "Lithium niobate *x*-cut, *y*-cut, and *z*-cut surfaces from *ab initio* theory," *Phys. Rev. B*, vol. 81, art. no. 214116, Jun. 2010.
[21] S. Sanna, G. Berth, W. Hahn, A. Widhalm, A. Zrenner, and W. G. Schmidt, "Vibrational properties of the $LiNbO_3$ z-surfaces," *IEEE Trans. Ultrason. Ferroeelectr. Freq. Control*, vol. 58, no. 9, pp. 1751–1756, 2011.
[22] S. R. Phillpot and V. Gopalan, "Coupled displacive and order–disorder dynamics in $LiNbO_3$ by molecular-dynamics simulation," *Appl. Phys. Lett.*, vol. 84, no. 11, pp. 1916–1918, 2004.
[23] I. V. Kityk, M. Makowska-Janusik, M. D. Fontana, M. Aillerie, and F. Abdi, "Band structure treatment of the influence of nonstoichiometric defects on optical properties in $LiNbO_3$," *J. Appl. Phys.*, vol. 90, no. 11, pp. 5542–5549, 2001.
[24] F. Bechstedt, in *Festköperprobleme/Advances in Solid State Physics*, U. Rössler, Ed., Braunschweig, Germany: Vieweg, 1992, vol. 32, p. 161.
[25] W. Y. Ching, Z.-Q. Gu, and Y.-N. Xu, "First-principles calculation of the electronic and optical properties of $LiNbO_3$," *Phys. Rev. B*, vol. 50, pp. 1992–1995, Jul. 1994.
[26] S. J. Jenkins, G. P. Srivastava, and J. C. Inkson, "Simple approach to self-energy corrections in semiconductors and insulators," *Phys. Rev. B*, vol. 48, pp. 4388–4397, Aug. 1993.
[27] F. Bechstedt, R. Del Sole, G. Cappellini, and L. Reining, "An efficient method for calculating quasiparticle energies in semiconductors," *Solid State Commun.*, vol. 84, no. 7, pp. 765–770, 1992.
[28] F. Bechstedt, K. Seino, P. H. Hahn, and W. G. Schmidt, "Quasiparticle bands and optical spectra of highly ionic crystals: AlN and NaCl," *Phys. Rev. B*, vol. 72, art. no. 245114, Dec. 2005.
[29] J. Seres, "Dispersion of second-order nonlinear optical coefficient," *Appl. Phys. B*, vol. 73, no. 7, pp. 705–709, 2001.
[30] A. M. Mamedov, H. Akkus, and S. Cabuk, "Linear and nonlinear optical susceptibilities in some ferroelectrics: *Ab-initio* calculation," *Int. J. Nanoelectron. Mater.*, vol. 3, no. 2, pp. 53–67, 2010.
[31] M. S. Hybertsen and S. G. Louie, "Electron correlation in semiconductors and insulators: Band gaps and quasiparticle energies," *Phys. Rev. B*, vol. 34, pp. 5390–5431, Oct. 1986.
[32] S. Albrecht, L. Reining, R. DelSole, and G. Onida, "*Ab initio* calculation of excitonic effects in the optical spectra of semiconductors," *Phys. Rev. Lett.*, vol. 80, pp. 4510–4153, May 1998.
[33] L. X. Benedict, E. L. Shirley, and R. B. Bohn, "Optical absorption of insulators and the electron-hole interaction: An *ab initio* calculation," *Phys. Rev. Lett.*, vol. 80, pp. 4514–4517, May 1998.
[34] M. Rohlfing and S. G. Louie, "Excitons and optical spectrum of the Si(111)-(2×1) surface," *Phys. Rev. Lett.*, vol. 83, pp. 856–859, Jul. 1999.
[35] L. J. Sham and T. M. Rice, "Many-particle derivation of the effective-mass equation for the Wannier exciton," *Phys. Rev.*, vol. 144, pp. 708–714, Apr. 1966.
[36] W. Hanke and L. J. Sham, "Local-field and excitonic effects in the optical spectrum of a covalent crystal," *Phys. Rev. B*, vol. 12, pp. 4501–4511, Nov. 1975.
[37] W. Hanke and L. J. Sham, "Many-particle effects in the optical spectrum of a semiconductor," *Phys. Rev. B*, vol. 21, pp. 4656–4673, May 1980.
[38] G. Kresse and J. Furthmüller, "Efficiency of *ab-initio* total energy calculations for metals and semiconductors using a plane-wave basis set," *Comput. Mater. Sci.*, vol. 6, pp. 15–50, Jul. 1996.
[39] G. Kresse and D. Joubert, "From ultrasoft pseudopotentials to the projector augmented-wave method," *Phys. Rev. B*, vol. 59, pp. 1758–1775, Jan. 1999.
[40] J. P. Perdew, J. A. Chevary, S. H. Vosko, K. A. Jackson, M. R. Pederson, D. J. Singh, and C. Fiolhais, "Atoms, molecules, solids, and surfaces: Applications of the generalized gradient approximation for exchange and correlation," *Phys. Rev. B*, vol. 46, pp. 6671–6687, Sep. 1992.
[41] M. Shishkin and G. Kresse, "Implementation and performance of the frequency-dependent *GW* method within the PAW framework," *Phys. Rev. B*, vol. 74, art. no. 035101, Jul. 2006.
[42] W. G. Schmidt, S. Glutsch, P. H. Hahn, and F. Bechstedt, "Efficient $O(N^2)$ method to solve the Bethe-Salpeter equation," *Phys. Rev. B*, vol. 67, art. no. 085307, Feb. 2003.
[43] P. H. Hahn, W. G. Schmidt, and F. Bechstedt, "Bulk excitonic effects in surface optical spectra," *Phys. Rev. Lett.*, vol. 88, no. 1, art. no. 016402, Jan. 2002.
[44] R. Leitsmann, W. G. Schmidt, P. H. Hahn, and F. Bechstedt, "Second-harmonic polarizability including electron-hole attraction from band-structure theory," *Phys. Rev. B*, vol. 71, art. no. 195209, May 2005.
[45] M.-Z. Huang and W. Y. Ching, "Calculation of optical excitations in cubic semiconductors. II. Second-harmonic generation," *Phys. Rev. B*, vol. 47, pp. 9464–9478, Apr. 1993.
[46] E. Luppi, H. Hübener, and V. Véniard, "Communications: *Ab initio* second-order nonlinear optics in solids," *J. Chem. Phys.*, vol. 132, no. 24, art. no. 241104, 2010.

Arthur Riefer was born in St. Petersburg, Russia, in 1985. He graduated in physics in Jena, Germany, in 2010. Currently, he is a Ph.D. student at Paderborn University. His research interests are linear and nonlinear optics, quasi-particle frameworks, computational physics, and ferroelectric and organic materials.

Simone Sanna was born in Cagliari, Italy, in 1977. He graduated in physics in 2003 and received his Ph.D. degree in physics in 2007. Since then, he has been a postdoctoral fellow at Paderborn University. His research interests are ferroelectrics and point defects.

Alexander V. Gavrilenko's photograph and biography were unavailable at time of publication.

Wolf Gero Schmidt was born in 1968. He studied physics in Jena, Germany. He graduated in physics in 1993 and received his Ph.D. degree in 1997. Since 2006, he has been a full professor of theoretical physics at Paderborn University. His research interests are the physics and chemistry of surfaces and interfaces, nanoscale science, and computational physics.